FLUTTER ANALYSIS OF LOW ASPECT RATIO WINGS

L. A. Parnell
Naval Ocean Systems Center, San Diego, CA

SUMMARY

Several very low aspect ratio flat-plate wing configurations are analyzed for their aerodynamic instability (flutter) characteristics. All of the wings investigated are delta planforms with clipped tips, made of aluminum alloy plate and cantilevered from the supporting vehicle body. Results of both subsonic and supersonic NASTRAN aeroelastic analyses as well as those from another version of the program implementing the supersonic linearized aerodynamic theory are presented. Results are selectively compared with published experimental data. Subsonic predictions are found to be reasonably consistent with the experimental data; however, supersonic predictions of the Mach Box method in NASTRAN are found to be erratic and erroneous, requiring the use of a separate program.

INTRODUCTION

Very low aspect-ratio wings are commonly used to control high speed missiles and new configurations of the wings are considered as missile designs are developed having different flight characteristics and design constraints than their predecessors. An analysis of the aeroelastic behavior of these wings is required to assure stable operation of the new configuration throughout the flight of the missile. This paper reports an evaluation of the aeroelasticity capabilities of NASTRAN in the performance of such an analysis. A thorough investigation is made of the flutter characteristics of two wing configurations, with results compared to published experimental data.

MODEL DESCRIPTION

The wings evaluated in this paper are of a flat-plate configuration with a clipped-tip delta planform and a large leading edge sweep angle. Two wing root chords were examined, having aspect ratios of 1.17 and 1.91, respectively. Aeroelastic instability was calculated throughout a wide Mach number range, both subsonic and supersonic. Both of the wings are assumed to be made of 6061 aluminum alloy plate with leading edges beveled as shown in figure 1. The presence of beveling was not included in the structural or aerodynamic models, however, as including such small details would have substantially increased the complexity of the finite element models with only modest improvement in the accuracy of the results.

Each wing evaluated in the investigation was modeled as a structure rigidly fixed at its line of intersection with the missile. Although such a model ignores the attachment flexibility which may be present at the root of the wing and neglects the strains which occur locally in the support shell, it can be shown that disregarding the additional flexibility provided by typical attachment methods has little effect on the predictions of the natural vibration (and, thus, flutter) characteristics of the wings. Similarly, the models idealize with little adverse effect the forward end of the leading edge of each wing as extending

to a point, rather than being truncated as is necessitated by typical wing attachment methods. Figure 2 shows the finite element mesh, Doublet-Lattice panel boxes (for the subsonic regime) and a typical Mach Box surface (for the supersonic regime) used in the analysis of one of the wings. The number and distribution of finite elements and panels changed with wing configuration and the Mach Box surfaces were different for each Mach number as well. Nevertheless, the diagrams in the figure are representative of all of the models generated in the investigation.

ANALYSIS PROCEDURE

Flutter analysis using the aeroelastic capabilities of the NASA Structural Analysis program, NASTRAN (ref. 1-3), begins with development and verification of a finite element structural model which will provide accurate normal vibration mode predictions. After giving consideration to the modeling limitations described in the previous section, the idealized structural finite element models were generated using undamped triangular and quadrilateral plate elements which have both bending and inplane stiffness and coupled mass matrices; the number and distribution of elements were selected to approximate equilateral triangles and unit-aspect-ratio quadrilaterals, as nearly as could be done practically. A fixed boundary at the wing roots and constraints on the remaining elements were employed to eliminate unimportant (inplane) vibration modes. Mode shapes and eigenvalues (natural frequencies) were determined by Givens' tridiagonal method (ref. 1,4). The validity of the resulting model's representation of the vibration modes and frequencies of actual delta wing structures was ascertained by comparing representative results with published experimental data. Appendix A presents such a comparison between predictions for the two wings considered in this paper and data from reference 5.

Having confirmation that the normal modes representation of the wings is accurate, the aerodynamic analysis proceeds by utilizing the eigenvectors as the generalized coordinates for the flutter solution; with NASTRAN, the analyst has a choice of the aerodynamic theory and the flutter method to be used. In this paper flutter in subsonic flow was predicted using the Doublet-Lattice aerodynamic theory and the usual American K-method of solving the dynamic aeroelastic stability problem. The supersonic problem was solved by means of the Mach Box program developed by Donato and Huhn (ref. 6), both as implemented in NASTRAN (ref. 3) and with another version of the program (ref. 7).

The definition of the Doublet-Lattice panel boxes is at the complete discretion of the analyst. Those shown in figure 2(b) typify the number and distribution used throughout this paper and follow recommended practice† that all aerodynamic boxes have an aspect ratio between one and two (and as close to unity as is practical). The Mach boxes, cf. figure 2(c), are determined by the analyst's choice of their spanwise number and by the requirement that each box have a diagonal parallel to the Mach line. Details of the aerodynamic computation are done internally by the computer codes, including actual generation of the aerodynamic grid points, computation of the steady and oscillatory air loads, transformation of the aerodynamic influence coefficients into modal coordinates and providing the interconnections between the aerodynamic and structural degrees of freedom through surface splines. The codes then generate numerical solutions to the linearized, three- dimensional unsteady perturbation potential flow equation, transform the results into physical coordinates and provide the pertinent output, viz. summaries providing flutter velocity (V_f) and frequency (F_f), artificial structural damping (g) and reduced frequency (k) for all modes, Mach numbers and air density ratios selected by the analyst. Plots showing velocity-damping and velocity-frequency curves are provided to assist in evaluation of the

† Aeroelasticity analysis conventions and recommendations were kindly provided by R. Ricketts and R. Doggett, Configuration Aeroelasticity Branch, NASA Langley Research Center.

results of the computations.

As the solution to the equation for modal flutter analysis is valid only when the artifical damping is zero (cf. ref. 1), tabular results must be interpolated for a given mode to determine values of k, V_f and F_f at the flutter point. Computations to determine the flutter velocity were repeated several times with different air density ratios (altitudes), and plotted against missile flight speeds in order to interpolate to the Match Point at a given Mach number, i.e., that air density ratio where the speed at which flutter occurs corresponds to the missile speed. The collection of these Match Points forms the flutter curve in which the subsonic and supersonic results may be joined by assuming a transonic dip in the flutter dynamic pressure, q_f , of 30% of the Mach 0.5 value to estimate q_f at the speed of sound. This curve is then compared with the missile flight envelope on a dynamic pressure vs. Mach number plot to determine the aerodynamic stability of a wing design when used on a given missile.

The theoretical predictions in this paper were evaluated in several ways to establish their validity. As the dynamic aeroelastic analysis approach implemented in NASTRAN for both subsonic and supersonic flow is the modal method, all results depend on accurate determination of the natural vibration modes of the structure and this was verified as mentioned previously. A check of the aerodynamic analysis procedures and computational results used for evaluation of the wings considered was made at the outset of the study by comparing NASTRAN flutter predictions with published experimental and theoretical results for a delta planform wing (ref. 8). Appendix B presents results of this comparison. Erratic behavior of the NASTRAN supersonic Mach Box predictions was subsequently noted, so the separate program of ref. 7 was used to repeat the analysis of the wings.

RESULTS AND DISCUSSION

The predicted behavior of the wings evaluated are summarized in tables I and II. The first five modal frequencies of each wing and the range of selected flutter parameters are listed in table I. A detailed summary of all the predicted flutter characteristics is listed in table II for each Mach number investigated. A plot of the dynamic pressure, q, as a function of Mach number for the theoretical flutter condition of both wing configurations is shown in figure 3. In this figure, all points plotted represent an instability condition. Flutter will occur at those Mach numbers where a flight envelope (plus a margin) drawn on the figure falls above the instability curve. As the nearly horizontal subsonic curves in figure 3 should have a positive slope, reflecting less dynamic pressure at the lower Mach numbers (cf. Appendix B), substantial unconservative errors in the Doublet-Lattice predictions are indicated there. Predictions of both the NASTRAN and ref. 7 implementations of the Mach Box program are shown in the figure and listed in table II. Although the NASTRAN Mach Box predictions are more conservative than those of ref. 7, the substantial differences (e.g., averaging 24.8% in q) and clearly erroneous results which were encountered at times in the analyses preclude the use of that NASTRAN procedure with any confidence until improvements are made in those computer routines.

It is instructive to note that flutter characteristics for wings having planforms similar to that considered in this paper can be inferred from presented results through the scaling law,

$$\frac{q}{q_o}\left(\frac{l}{l_o}\right)^4 = \frac{EI}{(EI)_o}.$$

This scaling law permits estimates of the flutter characteristics of wings having similar planforms to one of the configurations examined but having different materials, thicknesses or characteristic lengths. For

example, if a wing is made of a different gage material but is otherwise identical to a wing whose aerodynamic characteristics are known, the ratio of flutter dynamic pressures of the two wings would be proportional to the third power of their thickness ratio.

CONCLUDING REMARKS

The flutter analyses reported in this paper have demonstrated that the aeroelasticity capability is a powerful extension to the NASTRAN program's widely used structural and dynamics analysis procedures. Comparison of predictions with experimental data has verified that conventional modeling methods, analysis procedures and the NASTRAN computational routines have, in general, produced accurate predictions. The ease with which both structural and aeroelasticity analyses may proceed in conjunction with one another in the development of new aircraft or missile designs make the aeroelastic capability in NASTRAN a very convenient as well as useful feature of the program. However, the Mach Box program implementation in NASTRAN apparently has either errors or limitations in the algorithms which currently preclude recommending its use, at least for the low aspect ratio wing configurations examined in this paper.

SYMBOLS

A	aspect ratio of wing
b	root chord, cm
c	velocity of sound, m/s
D	flexural rigidity, Nm
E	modulus of elasticity, kPa
f	frequency, Hz
g	artificial damping
I	moment of inertia, cm^4
k	reduced frequency ($\omega b/2V$)
l	semi-span of wing, cm
M	Mach number
q	dynamic pressure, Pa
t	wing thickness, cm
V	velocity, m/s
γ	density of wing material, Kg/m^3
Δ	relative difference
Δl	length of wing clipped, cm
μ	Poisson's ratio
ρ	air density, Kg/m^3
ω	wing circular frequency, 1/s

Subscripts

f	flutter
n	mode number
o	reference value

REFERENCES

1. "The NASTRAN Theoretical Manual," SP-221(05), NASA Scientific and Technical Information Office, Washington, D.C., June 1985.

2. "The NASTRAN User's Manual," SP-222(05), NASA Scientific and Technical Information Office, Washington, D.C., January 1981.

3. Rodden, W.P., R.L. Harder and E.D. Bellinger, "Aeroelastic Addition to NASTRAN," NASA CR-3094, March 1979.

4. Givens, W. "Numerical Computation of the Characteristic Values of a Real Symmetric Matrix," Oak Ridge National Lab., ORNL-1574, 1954.

5. Gustafson, P.N., W.F. Stokey and C.F. Zorowski, "The Effect of Tip Removal on the Natural Vibrations of Uniform Cantilevered Triangular Plates", J. Aeronaut. Sci, 21:621 (1954).

6. Donato, V.W. and C.R. Huhn, Jr., "Supersonic Unsteady Aerodynamics for Wings with Trailing Edge Control Surfaces and Folded Tips," Air Force Flight Dynamics Lab., AFFDL-TR-68-30, August 1968.

7. "MBOXTI", the AFFDL MBOX computer code with revisions and updates by Texas Instruments, Inc. and E.L. Jeter, Naval Weapons Center, China Lake, CA, 1984.

8. Hanson, P.W. and G.M. Levey, "Experimental and Calculated Results of a Flutter Investigation of Some Very Low Aspect-Ratio Flat-Plate Surfaces at Mach Numbers from 0.62 to 3.00," NASA TN D-2038, 1963.

APPENDIX A. NORMAL MODES OF WINGS A AND B

In order to determine the accuracy of normal mode calculations for the wings evaluated in this paper, predictions are compared with known characteristics of built-in, clipped triangular plates. Using the procedures described in reference 5, the unknown modal frequencies of a plate with planform similar to that of one whose vibration characteristics have been experimentally determined are given by

$$\omega' = \omega_D \sqrt{D' / (\gamma' t' l_o'^4)} \qquad \text{(A-1)}$$

where primed quantities refer to the plate in question and unprimed to the known reference plate. In equation (A-1) $\omega_D = \omega \sqrt{\gamma t l_o^4 / D}$ is the dimensionless angular frequency of the plate based on its semi-span and flexural rigidity, $D = Et^3/[12(1-\mu^2)]$. Frequency data and mode shapes are presented in reference 5 for plates with aspect ratios of 2 and 4 having clipping fractions, $\Delta l/l_o$, between zero (full triangle) and 0.4. As that work reports linear variation in natural frequency with aspect ratio and good results when interpolating between clipping fractions, characteristics of both wings examined in this paper may be inferred from the published data. The procedure consists of utilizing curves of frequency shift, $\Delta\omega/\omega$, as a function of clipping fraction to interpolate the experimental data to the amount of clipping for the wings evaluated, followed by interpolation between unclipped aspect ratios to the actual

wing configuration. For wing B the clipping fraction is $\Delta l/l_o = 0.270$ and the unclipped aspect ratio is $A_o = 2.038$. Table A-I shows interpolation of the experimental data to these characteristics.

Comparing the interpolated data from reference 5 with the results of the finite element model shows less than 5% error in the NASTRAN frequency predictions for the five modes used in the flutter analysis, as listed in table A-II(b). The mode shapes (eigenvectors) determined by the NASTRAN analysis are presented in figure A in the form of contour plots. Comparing these predictions with the mode line photographs of reference 5 shows excellent agreement and completes validation of the finite element model used for modal formulation of the aerodynamic instability analysis.

A similar interpolation of experimental data of reference 5 to the configuration of wing A is given in tables A-III and A-II(a). The NASTRAN predictions are not as good as in the wing B configuration, showing up to 9% deviation from experimental results. This larger error is due to the use of a coarser grid of elements for the wing A model (21 total elements) than for the wing B model (45 total elements). These errors are, however, small enough to validate use of the finite element model used in the flutter analysis of wing B.

APPENDIX B. COMPARISON OF NASTRAN PREDICTIONS WITH EXPERIMENTAL FLUTTER CHARACTERISTICS OF A NASA WING.

As a means of verifying the validity of the procedures used in this paper, a flutter analysis was performed on a delta wing whose measured characteristics were reported in reference 8. Model 1A of that reference was evaluated for both subsonic and supersonic flutter conditions using the NASTRAN Doublet-Lattice and Mach Box methods, respectively. Figure B-1 shows the model geometry and reported node lines for the model. Modal results for the triangular plate were obtained using an 18-element matrix composed of 15 quadrilateral and 3 triangular elements. Table B-I presents a comparison of experimental and predicted modal frequencies for the model.

The aeroelastic instability analyses used 48 Doublet-Lattice panel boxes for subsonic flow and 20 chordwise Mach boxes for supersonic flow (the number of spanwise boxes being determined by Mach number). Numerical results were obtained using the same methodology as was employed in the remainder of this paper. They are compared with the experimental data of reference 8 in table B-II and plotted in figure B-2. Although these comparisons show substantial predictive errors, those in the important parameter of flutter dynamic pressure, q, are acceptable. The error is large only at the lowest Mach number examined. For the highest (and most critical) Mach number compared, excellent agreement occurs in this parameter, especially when the rather poor modal results (shown in table B-I) are considered.

As the modal comparisons used in the body of this paper are substantially better than those shown in this appendix, the aeroelasticity predictions may be expected to be correspondingly improved. In addition, even though the errors in the dynamic pressure predictions in this appendix are large at times, they are, with the exceptions of the lowest speed condition, well within the flutter margin normally imposed on vehicle flight envelopes. The large low-speed error is an unconservative instability prediction in this regime and indicates that the nearly horizontal theoretical curves shown in figure 3 should show a reduction at the lower Mach numbers.

TABLE I. MODAL FREQUENCIES AND FLUTTER ANALYSIS CONDITIONS

Wing	Modal Frequencies (Hz)					Range of Flutter Conditions		
	f_1	f_2	f_3	f_4	f_5	M	ρ/ρ_o	F_f(Hz)
A	203.5	560.7	1118	1167	1887	.50 - 1.75	9.47 - 14.1	362.8 - 824.5
B	140.1	310.3	590.7	815.5	996.1	.50 - 2.00	3.09 - 9.55	202.3 - 243.3

TABLE II. THEORETICAL FLUTTER PREDICTIONS

Wing	M	Flutter Conditions †					
		ρ/ρ_o	k	V (m/s)	q (MPa)	c (m/s)	f_f (Hz)
A	0.50	14.1	1.082	456	1.794	911	442.1
	0.60	12.2	0.967	497	1.843	828	430.0
	0.70	10.9	0.858	538	1.926	768	412.7
	0.80	9.80	0.754	579	2.040	724	390.3
	0.90	9.07	0.653	622	2.149	691	362.8
	1.20	6.92	0.929	716	2.176	597	600.4
	1.50	8.32	0.825	991	5.003	660	730.1
	1.75	9.47	0.744	1240	8.931	709	824.5
B	0.50	9.55	0.956	357	0.744	713	237.7
	0.60	8.05	0.864	388	0.743	647	233.2
	0.70	6.93	0.776	419	0.746	599	226.5
	0.80	6.14	0.693	451	0.766	564	216.7
	0.90	5.50	0.604	482	0.782	535	202.3
	1.50	3.76	0.978	691	1.099	461	235.5
	1.75	3.40	0.886	779	1.267	445	240.5
	2.00	3.09	0.811	864	1.411	431	243.3
B (NASTRAN)	1.50	3.26	0.36	658	0.866	439	
	1.75	2.76	0.32	728	0.898	416	
	2.00	2.63	0.28	815	1.072	408	

† Subsonic predictions obtained from NASTRAN (ref. 1-3), supersonic from ref. 7 except as noted.

TABLE A-I. NORMAL MODES OF WING B

(a) Determination of Frequency Shifts for the Specific Clipping Fraction.

Mode	ω''_D ($\frac{\Delta l}{l} = 0$) †		$\frac{\Delta\omega}{\omega_o}$ ($\frac{\Delta l}{l} = 0.270$) ††		ω''_D ($\frac{\Delta l}{l} = 0.270$)	
	Series I	Series II	Series I	Series II	Series I	Series II
1	5.50	5.87	.339	.379	7.365	8.095
2	14.7	23.8	.186	.172	17.43	27.89
3	27.5	32.4	.539	.331	42.32	43.12
4	29.8	56.1	.036	.166	30.87	65.41
5	46.5	76.0	.090	.366	50.68	103.82
6	57.0	99.7	.068	.103	60.88	109.97

Aspect ratio of unclipped plates: A_o = 2 (Series I), 4 (Series II).

† Data from Tables 1 and 3, reference 5.
†† Taken from Figures 8 and 9, reference 5.

(b) Interpolation Between (Unclipped) Aspect Ratios.

Mode	ω''_D *	Wing B **	
		ω''_B	f_B
1	7.38	852	136
2	17.6	2036	324
3	42.3	4888	778
4	31.5	3640	579
5	51.7	5969	950
6	61.8	7137	1136

* $\omega''_{D_n} = \omega''_{D_{I_n}} + \frac{0.038}{2.0}(\omega''_{D_{II_n}} - \omega''_{D_{I_n}})$

** $\omega''_B = \omega''_D \sqrt{D / \gamma h l_o^4} = 115.5\omega''_D$, $f_B = \frac{\omega''}{2\pi} = 18.38\omega''_D$

TABLE A-II. COMPARISON OF NATURAL MODES OF LOW ASPECT RATIO WINGS

(a) Wing A.

Mode	Frequency (Hz)		
	Experimental †	NASTRAN *	Δ (%)
1	202	203.5	-0.74
2	543	560.7	-3.2
3	1040	1118.0	-7.0
4	1094	1167.4	-6.3
5	1719	1886.7	-8.9
6	2096	2323.7	-9.8

(b) Wing B.

Mode	Frequency (Hz)		
	Experimental †	NASTRAN *	Δ (%)
1	136	140.1	-2.9
2	324	310.3	4.4
3	579	590.7	-2.0
4	778	815.5	-4.6
5	950	996.1	-4.6
6	1136	1213.	-6.3

† As interpolated from data of reference 5 to the configuration (aspect ratio and clipping fraction), dimensions and materials of the wings examined.

* Using Givens method with coupled mass matrices. A total of 21 elements were used for wing A, 45 for wing B.

TABLE A-III. NORMAL MODES OF WING A

(a) Determination of Frequency Shifts for the Specific Clipping Fraction.

Mode	$\omega^{\sim}_D$ ($\frac{\Delta l}{l} = 0$) †		$\frac{\Delta\omega}{\omega}$ ($\frac{\Delta l}{l} = 0.061$) ††		$\omega^{\sim}_D$ ($\frac{\Delta l}{l} = 0.061$)	
	Series I	Series II	Series I	Series II	Series I	Series II
1	5.50	5.87	.017	.042	5.59	6.116
2	14.7	23.8	.011	.022	14.86	24.32
3	27.5	32.4	.045	.022	28.74	33.11
4	29.8	56.1	0.0	.011	29.8	56.72
5	46.5	76.0	.011	.056	47.01	80.26
6	57.0	99.7	.005	0.0	57.28	99.7

Aspect ratio of unclipped plates: A_o = 2 (Series I), 4 (Series II).

† Data from Tables 1 and 3, reference 5.
†† Taken from Figures 8 and 9, reference 5.

(b) Interpolation Between (Unclipped) Aspect Ratios.

Mode	$\omega^{\sim}_D$ *	Wing A **	
		$\omega^{\sim}_A$	f_A
1	5.60	1270.	202.
2	15.0	3410.	543.
3	28.8	6534.	1040.
4	30.3	6872.	1094.
5	47.6	10801.	1719.
6	58.1	13169.	2096.

* $\omega^{\sim}_{D_n} = \omega^{\sim}_{D_{I_n}} + \frac{0.038}{2.0} (\omega^{\sim}_{D_{II_n}} - \omega^{\sim}_{D_{I_n}})$

** $\omega^{\sim}_A = \omega^{\sim}_D \sqrt{D / \gamma h l_o^4} = 226.7 \omega^{\sim}_D$, $\quad f_A = \frac{\omega^{\sim}_A}{2\pi} = 36.07\, \omega^{\sim}_D$

TABLE B-I. FREQUENCY COMPARISONS WITH A NASA DELTA-WING MODEL

(a) Selected Experimental Frequencies (from Ref. 8, Table I, Model 1A).

M	Frequency (Hz)			
	F_1	F_2	F_3	F_4
0.64	72	171	320	367
0.79	79	193	350	396
1.30	75	120	305	367
2.00	75	173	320	379

(b) Natural Frequency Comparison.

Mode	Frequency (Hz)		
	Experimental †	NASTSRAN ††	Δ(%)
1	75.2	85.9	14.2
2	176.8	209.2	18.4
3	323.8	389.2	20.2
4	377.2	475.4	26.0

† Average of data in table (a). †† Using 18 elements.

TABLE B-II. FLUTTER CHARACTERISTICS OF A NASA DELTA WING MODEL

M	Experimental Results †			NASTRAN Predictions ††			Δ(%)		
	ρ/ρ_o	q (kPa)	f_f	ρ/ρ_o	q (kPa)	f_f	ρ/ρ_o	q	f_f
0.64	0.6064	16.9	150	0.8621	24.3	165	42.2	43.2	9.9
0.79	0.6186	25.5	150	0.6350	25.6	154	2.7	0.6	2.5
1.30	0.3305	30.8	150	0.2801	25.5	104	-15.2	-17.3	-30.5
2.00	0.2489	40.5	153	0.2061	44.3	110	-17.2	9.3	-27.8

† From Table I Model 1A of ref. 8.

†† Using modal results shown in Table B-I, 48 Doublet-Lattice panel boxes (for subsonic predictions) and 20 chord-wise Mach boxes (for supersonic predictions).

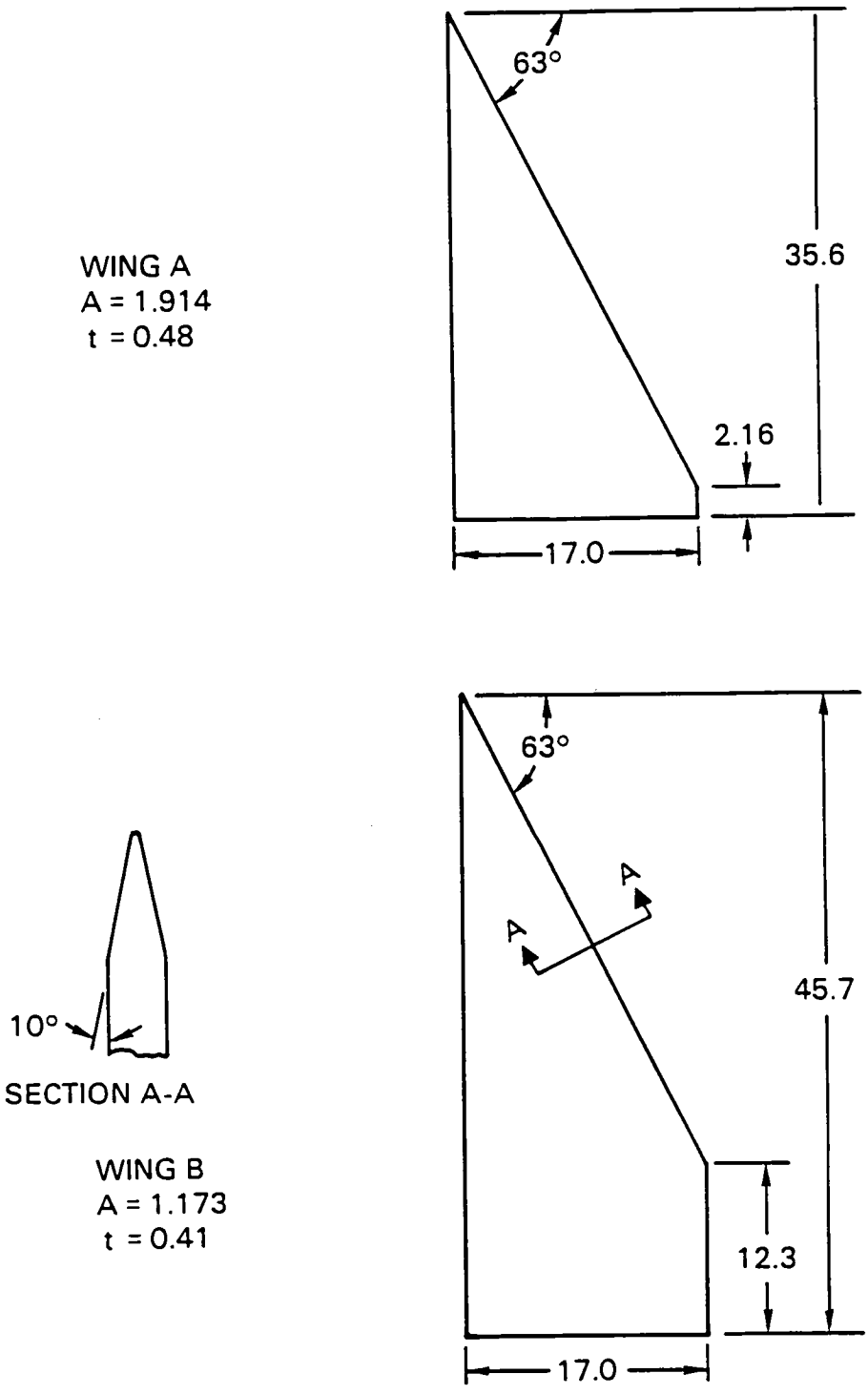

Figure 1. Wing geometries.

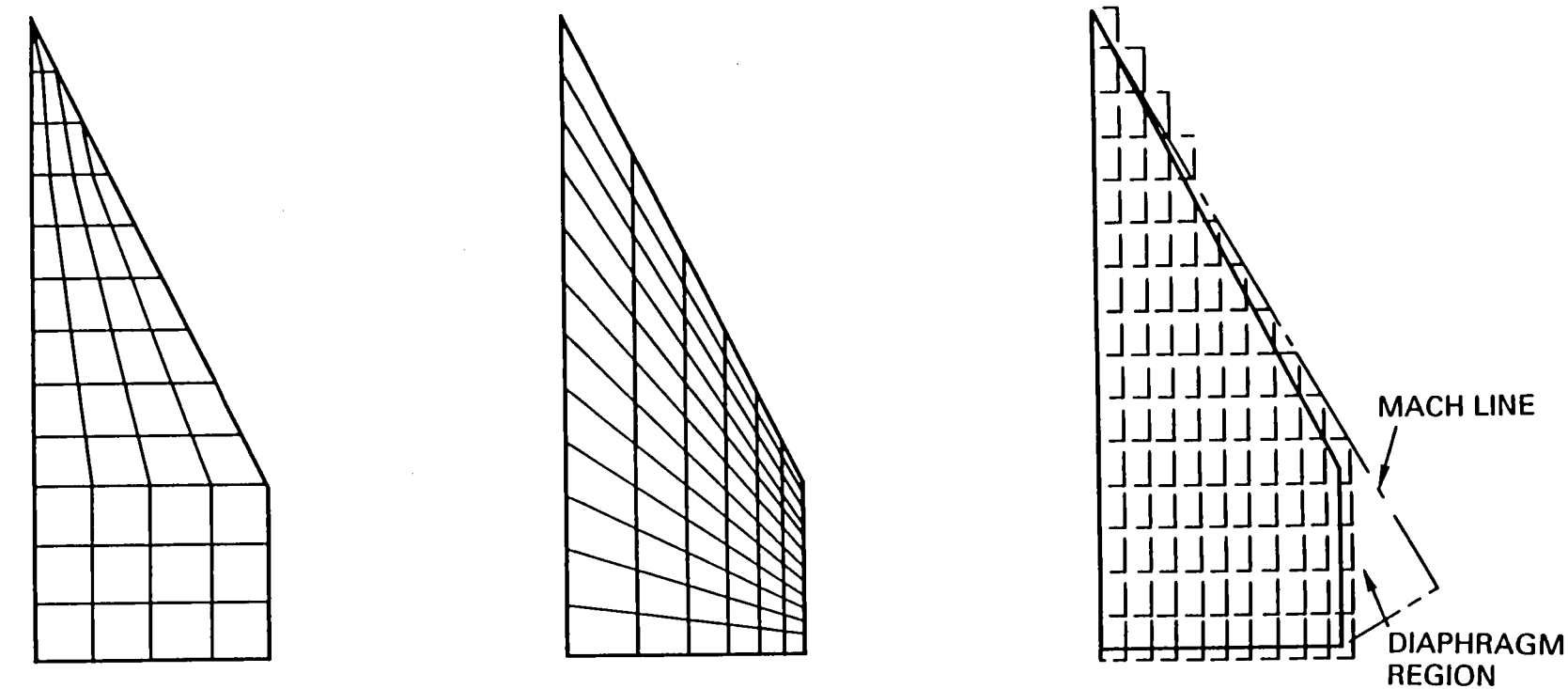

(a) FINITE ELEMENTS

(b) DOUBLET-LATTICE PANEL BOXES

(c) MACH BOXES (M = 2.0)

Figure 2. Wing B model characteristics.

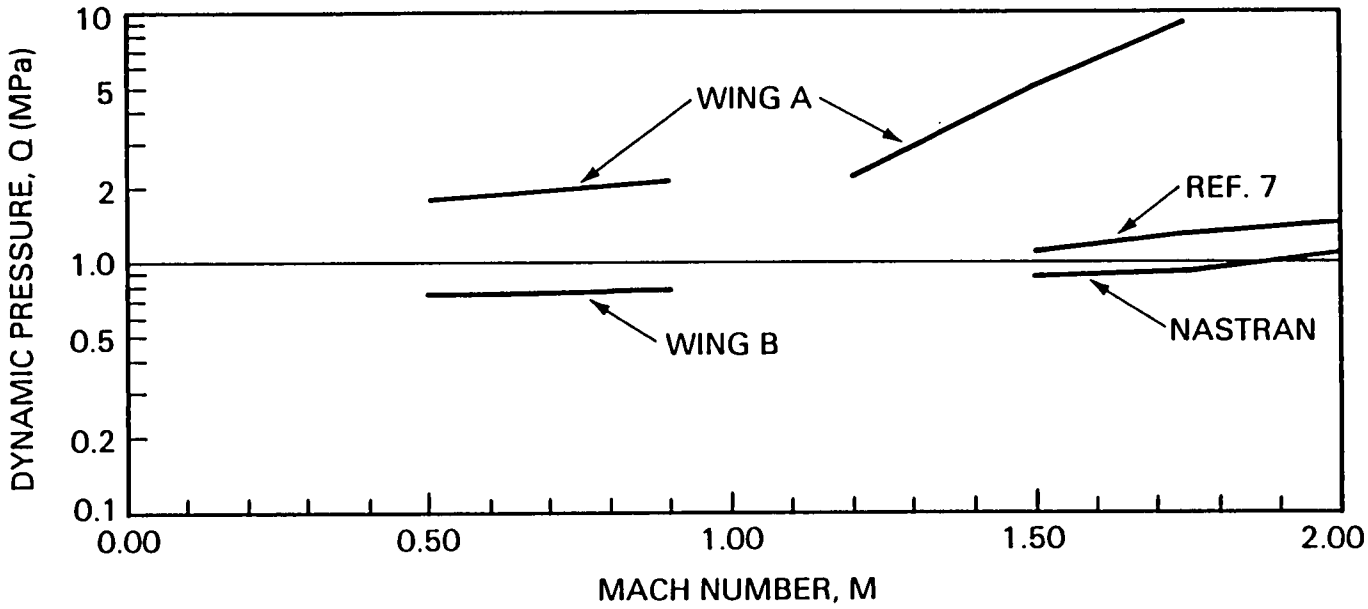

Figure 3. Flutter characteristics of wings A, B.

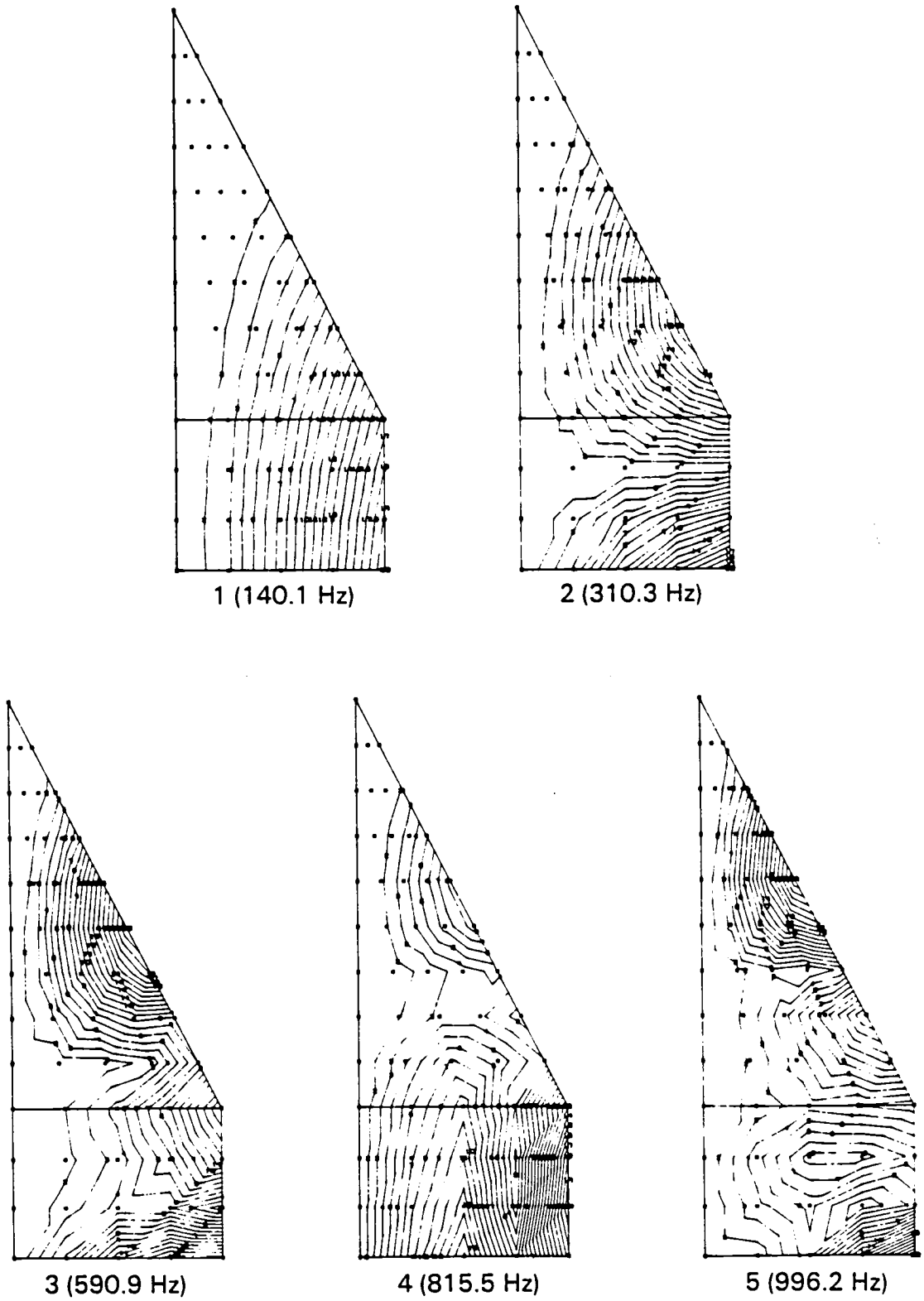

Figure A. Mode shapes and frequencies of Wing B as predicted by NASTRAN.

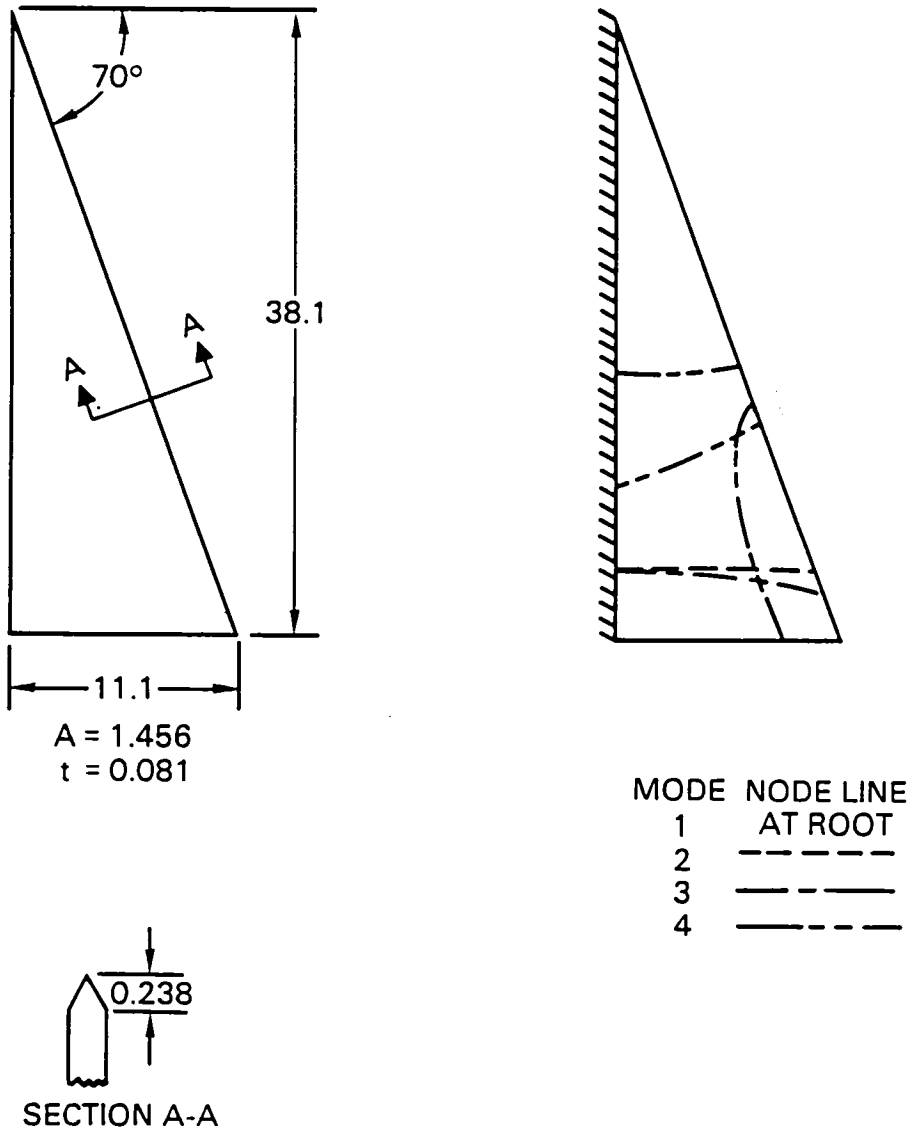

Figure B-1. Geometry and node lines for model 1A of reference 8.

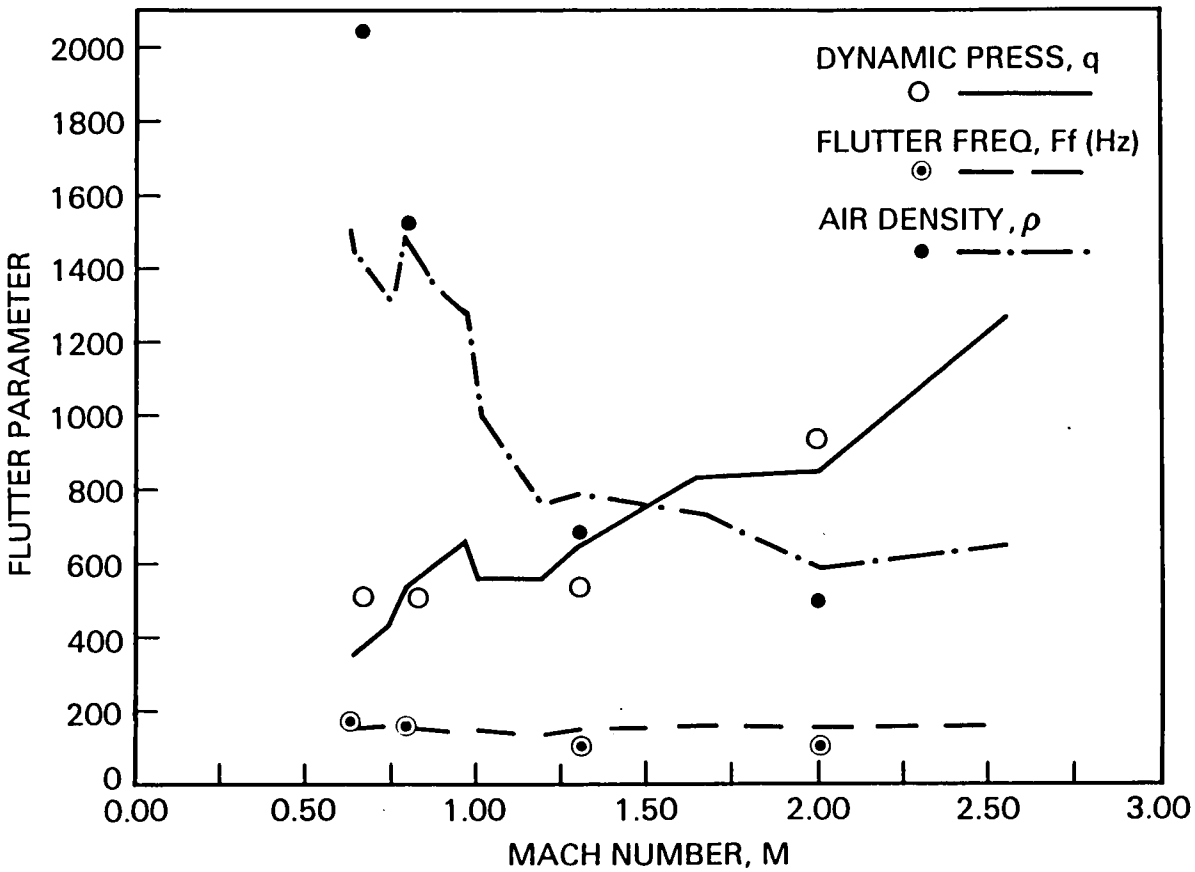

Figure B-2. Flutter characteristics of a NASA delta-wing model. Lines are experimental data of reference 8. Symbols are NASTRAN predictions.